

formaldehyde or with the noncapsulated M7 strain [D. S. Stephens, J. S. Swartley, S. Kathariou, S. A. Morse, *Infect. Immun.* **59**, 4097 (1991)]. Immunoglobulin titers were expressed as the reciprocal of serum dilution that gave an  $A_{490}$  value of 0.4 above the preimmune sera. We prepared immunoblots on purified proteins, OMVs, or total cell extracts with 15% polyacrylamide gels and 1:200 sera dilutions. We evaluated serum bactericidal activity against strains 2996 and BZ232, as described [C. C. A. C. Peeters *et al.*, *Vaccine* **17**, 2702 (1999)], with pooled baby rabbit serum used as complement source (Cedar Lane). The serum bactericidal titers were reported as the reciprocal of the serum dilution yielding  $\geq 50\%$  bacterial killing. We tested serum bactericidal activity with human complement, as described [R. E. Mandrell, F. H. Azmi, D. M. Granoff, *J. Infect. Dis.* **172**, 1279 (1995)], against strains 8047 (obtained from W. Zollinger), M986 [D. A. Caugant *et al.*, *J. Bacteriol.* **169**, 2781 (1987)], and NGP165 (17)—the strains in our collection that could be tested with our human complement source. The noncapsulated M7 strain or capsulated strains whose capsule had been permeabilized by treatment with 70% ethanol at  $-20^{\circ}\text{C}$  for 1 hour were analyzed for cell-bound fluorescence with a FAC-Scan flow cytometer. We used R-phycoerythrin-conjugated goat F(ab)<sub>2</sub> antibody to mouse immunoglobulin (Jackson ImmunoResearch) to detect antibody binding.

15. I. Goldschneider, E. C. Gotschlich, M. S. Artenstein, *J. Exp. Med.* **129**, 1307 (1969).
16. M. C. J. Maiden *et al.*, *Proc. Natl. Acad. Sci. U.S.A.* **95**, 3140 (1998).
17. A. Seiler, R. Reinhardt, J. Sarkari, D. A. Caugant, M. Achtman, *Mol. Microbiol.* **19**, 841 (1996).
18. J. Wang, D. A. Caugant, G. Morelli, B. Koumare, M. Achtman, *J. Infect. Dis.* **167**, 1320 (1993).
19. Gene variability: *Neisseria* strains. Twenty-two *N. meningitidis* serogroup B strains have been used for gene variability analyses: NG6/88, BZ198, NG3/88, 297-0, 1000, BZ147, BZ169, 528, NGP165, BZ133, NGE31, NGF26, NGE28, NGH38, SWZ107, NGH15, NGH36, BZ232, BZ83, H44/76 (17), MC58 [B. T. McGuinness *et al.*, *Lancet* **337**, 514 (1991) (17)], and 2996 (13); three serogroup A strains: 205900 and F6124 (our collection) and Z2491 (16) (sequenced at The Sanger Centre); two serogroup C strains: 90/18311 (18) and 93/4286 (16); one strain of each serogroup W, X, Z, and Y—A22, E26, 860800, and E32, respectively (16); one strain of *N. cinerea* (our collection); one strain of *N. lactamica* (our collection); and three strains of *N. gonorrhoeae*—Ng F62 and Ng SN4 (our collection) and FA1090 [J. A. Dempsey, W. Litaker, A. Madhure, T. L. Snodgrass, J. G. Cannon, *J. Bacteriol.* **173**, 5476 (1991); sequenced at The Oklahoma University]. We amplified selected genes by PCR with the following primers mapping about 70 base pairs upstream and downstream from the coding regions. *gna33*, TCGGCCCTGTGTTAAATCCCCCT (Forward), GGTATCGCAAAAATTCGCTTAATGCG (Reverse); *gna992*, GTTGGGGGAATTATCAGAAAACCC (Forward), GGCTCAGCGGCAATCCG (Reverse); *gna1162*, AGAGAAAAGGCTGTTCCCG (Forward), CTTGCAAGTATCAAGATTCGCG (Reverse); *gna1220*, TTGAACAGGAAACCGCGCC (Forward), TATTTGAAGCGGAATACAACCTTGCCC (Reverse), TATTTGAAGCGGAATACAACCTGTTCCG (Reverse for gonococcus); *gna1946*, CGAATCCGACGGCAGGACTC (Forward), GGCGAGGAAATGGCGGATTAAG (Reverse); *gna2001*, CAATCAACAAGATATTTTCGACTG (Forward), TTTGACCTTTTCGGTACAGG (Reverse); *gna2132*, GCGTTCAGACGGCA-TATTTTAC (Forward), GGTTTATCAACTGATCGCGACTTGA (Reverse), TTGGGATGCCGCTTTTCGG (Reverse for gonococcus); *porA*, TATCGGTTGTTG-CCGATGTTTATAGG (Forward), TGGGCTGAAG-CAGATTGGCAGTACG (Reverse). We used about 10 ng of chromosomal DNA as template. PCR products were purified and sequenced by primer walking on both strands. To study the frequency of recombination among closely related nucleotide sequences, we used the homoplasmy test ([ftp://novell-del-valle.molgen.mpg.de](http://novell-del-valle.molgen.mpg.de)), which was designed to estimate the significance of convergent mutations in a phylogenetic tree by comparing the expected and observed value of homoplasies, being 0 for a clonal population

and 1 for complete linkage equilibrium. We applied the test to the seven selected genes (or selected conserved regions), using in each case only different allele sequences. The data reported were obtained as described (21), using no outgroup and considering a medium level of expression for all the genes. The values of the H ratio obtained were, respectively, 0.005 for *gna1946*, 0.065 for *gna2001*, 0.133 for *gna1162*, 0.251 for *gna1220*, 0.302 for the 3'-end of *gna992*, and 0.524 for *gna33*, which give a geometric mean of 0.11. This is lower than the value previously reported for conserved meningococcal housekeeping genes [S. Suerbaum *et al.*, *Proc. Natl. Acad. Sci. U.S.A.* **95**, 12619 (1998)]. *gna2132*, which, even in the conserved 3'-end, gave an H ratio of 0.707, indicating high levels of recombination, was not included in the analysis.

20. A. Bart, J. Dankert, A. van der Ende, *Infect. Immun.* **67**, 3842 (1999).
21. J. Maynard Smith and N. H. Smith, *Mol. Biol. Evol.* **15**, 590 (1998).
22. J. Lommatzsch, M. F. Templin, A. R. Kraft, W. Vollmer, J.-V. Holtje, *J. Bacteriol.* **179**, 5465 (1997); J. V. Holtje, *Microbiol. Mol. Biol. Rev.* **62**, 181 (1998).
23. M. Piza *et al.*, data not shown.
24. N. Saitou and M. Nei, *Mol. Biol. Evol.* **4**, 406, 1987.
25. M. Kimura, *J. Mol. Evol.* **16**, 111, 1980.
26. J. St. Geme III, D. Cutter, S. J. Barenkamp, *J. Bacteriol.* **178**, 6281 (1996); D. A. Relman, M. Domenighini, E. Toumanen, R. Rappuoli, S. Falkow, *Proc. Natl. Acad. Sci. U.S.A.* **86**, 2637 (1989).

27. M. Chanyangam, A. L. Smith, S. L. Moseley, M. Kuehn, P. Jenny, *Infect. Immun.* **59**, 600 (1991).
28. M. D. Wuenschel, S. Kohler, A. Bubert, U. Gerike, W. Goebel, *J. Bacteriol.* **175**, 3491 (1993).
29. Author contributions were as follows: experimental, M. Piza; computer, V. Scarlato; coordination, G. Grandi; computer analysis, V. Massignani, M. Scarselli, M. Mora, C. L. Galeotti, and G. Ratti; gene expression, B. Aricò, M. Comanducci, B. Capecci, L. Baldi, E. Storni, M. Broeker, B. Knapp, and E. Hundt; gene variability, M. Comanducci and B. Capecci; sera analysis, M. M. Giuliani, L. Santini, E. Luzzi, and E. Bartolini; help with FACS analysis, S. Nuti; protein purification, G. T. Jennings, S. Savino, E. Marchetti, P. Zuo, and R. Manetti; nucleotide sequencing, E. Blair, T. Mason, and H. Tettelin; help with project planning and sequence annotation, E. R. Moxon, N. J. Saunders, D. Hood, and A. C. Jeffries; help with project planning and bactericidal assays, D. M. Granoff. We thank M. Achtman and F. Frati for useful discussions; B. Brunelli, D. Serruto, and D. Veggi for technical help; and J. Adu-Bobie for sharing unpublished observations. We also acknowledge the Gonococcal Genome Sequencing Project (B. A. Roe, S. P. Lin, L. Song, X. Yuan, S. Clifton, T. Ducey, L. Lewis, and D. W. Dyer) at The University of Oklahoma and the *N. meningitidis* Sequencing Group at the Sanger Centre. Finally, we thank C. Mallia for editing, G. Corsi for artwork, and D. Kingsbury for support and advice.

25 October 1999; accepted 27 January 2000

## gridlock, an HLH Gene Required for Assembly of the Aorta in Zebrafish

Tao P. Zhong,\* Michael Rosenberg,\*† Manzoor-Ali P. K. Mohideen,‡ Brant Weinstein,§ Mark C. Fishman||

The first artery and vein of the vertebrate embryo assemble in the trunk by migration and coalescence of angioblasts to form endothelial tubes. The *gridlock* (*grl*) mutation in zebrafish selectively perturbs assembly of the artery (the aorta). Here it is shown that *grl* encodes a basic helix-loop-helix (bHLH) protein belonging to the Hairy/Enhancer of the split family of bHLH proteins. The *grl* gene is expressed in lateral plate mesoderm before vessel formation, and thereafter in the aorta and not in the vein. These results suggest that the arterial endothelial identity is established even before the onset of blood flow and implicate the *grl* gene in assignment of vessel-specific cell fate.

Arteries and veins are morphologically and functionally very distinct. For example, arteries deliver oxygenated blood at high pressure from the heart, whereas veins serve as capacitance vessels for blood return. Some of the morphological differences may be imposed

after, and depend upon, onset of function. However, a complete vascular loop, composed of the trunk dorsal aorta and posterior cardinal vein, is needed to accommodate the output of the first heartbeat. These simple tubes of endothelium form by local aggregation of angioblasts, a process termed vasculogenesis (1). Neither mutations nor molecular markers have revealed whether there are arterial-venous distinctions between angioblast progenitors. In the mouse, ephrinB2 is selectively expressed on the arteries and EphB3 and EphB4 on the veins, but this occurs after vasculogenesis (2). Furthermore, mutation of ephrinB2 does not affect vasculogenesis, although it does disrupt later vessel formation and remodeling, a process termed angiogenesis (2).

The gridlock mutation (*grl*<sup>m145</sup>) was originally isolated in a large-scale chemical mu-

Cardiovascular Research Center, Massachusetts General Hospital—Harvard Medical School, 149 13th Street, 4th floor, Charlestown, MA 02129, USA.

\*These authors contributed equally to this work.

†Present address: Aventis Pharma, 26 Landsdowne Street, Cambridge, MA 02139, USA.

‡Present address: Jake Gittlen Cancer Research Institute, Pennsylvania State University College of Medicine, 500 University Drive, Hershey, PA 17033, USA.

§Present address: Unit on Vertebrate Organogenesis, Laboratory of Molecular Genetics, National Institute of Child Health and Human Development, Building 6B, 6 Center Drive, Bethesda, MD 20892, USA.

||To whom correspondence should be addressed. E-mail: fishman@cvcrc.mgh.harvard.edu

REPORTS

tagenesis screen (3) for developmental mutations of the zebrafish, *Danio rerio*. Homozygous mutant embryos have no circulation to the posterior trunk and tail because of a lo-

calized block to caudal blood flow at the base of the dorsal aorta, the region where the two anterior lateral dorsal aortae merge to form the single midline dorsal aorta. Cranial ves-

sels and other trunk vessels appear to form normally in the mutants.

To clone the *grl* mutation, we first established its position on the genetic map, using

**Fig. 1.** The integrated genetic, physical, and radiation hybrid maps of the zebrafish *gridlock* region. Marker z536 was linked to the *gridlock* locus on chromosome 20 by bulked segregant analysis and used to initiate a chromosomal walk. Five and 12 recombinants were identified with z536 and z9794, respectively, among 1200 mutants. A YAC contig was constructed spanning about 2 Mb of the *grl* region. The YAC sizes (from 350 kb to 1.5 Mb) were determined by pulsed-field gel electrophoresis. The BAC/PAC contig was assembled from three BACs and three PACs with the T3 end of YAC133 as a starting point. G, H, I, J, K, and L correspond to YAC, BAC, and PAC ends. The number of recombinants between the markers and *grl* locus are shown below the Chromosome line. Both PAC14 and BAC14 were shotgun-sequenced, providing fivefold DNA sequence coverage of each. The five exons of *grl* were identified by sequence analysis. Some of the genetic markers were placed on a radiation hybrid (RH) map to integrate genetic, physical, and RH maps in the mutation region, as shown. The distance in centirays (cR) between these markers on the RH map is indicated below the Radiation Hybrid line. The YAC sizes are not proportional to the scale bar.

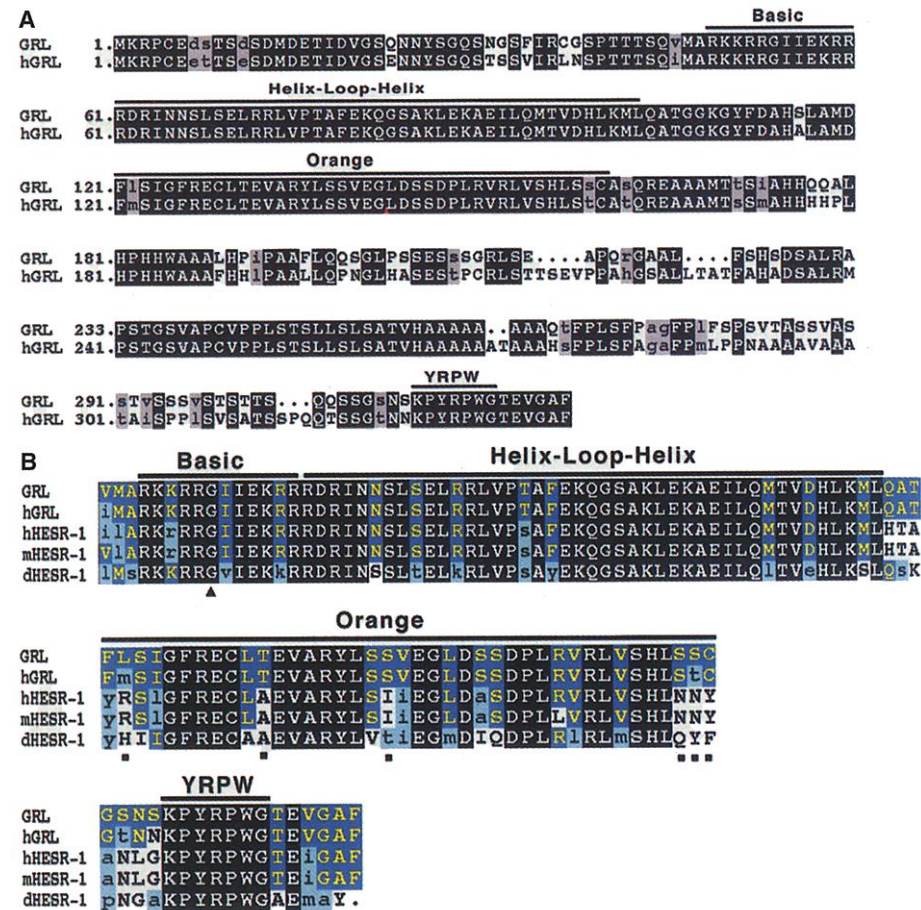
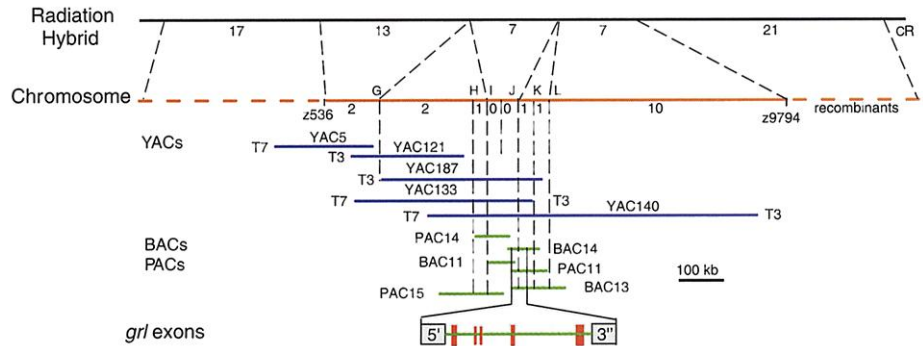


**Fig. 2.** Sequence and domain structure of the zebrafish and human Grl proteins, sequence alignment of Grl with other Hesr proteins, and the position of the point mutation in the zebrafish *grl* mutant allele. (A) Amino acid sequence alignment of zebrafish Grl and human GRL. The human GRL sequence was assembled from human expressed sequence tags (AF727779 and AA116067). bHLH, Orange, and YRPW domains are indicated above the alignment. Black boxes, amino acid identity. Gray boxes, amino acid similarity. The GenBank accession numbers for Grl and hGRL are AF237948 and AF237949, respectively. (B) Sequence comparison of Grl with other Hesr proteins in the bHLH domain, Orange domain, and COOH-terminal motif. Black box, amino acid identity among all Grl and Hesr proteins. Dark blue boxes, amino acids that are distinct for Grl proteins and different from Hesr proteins. The Orange domain differences are shown as black squares below the sequences. Light blue boxes, amino acid similarity among all Grl and Hesr proteins. Black triangles, Pro→Gly substitution in the basic region of bHLH and Trp→Tyr substitution in the protein-protein interaction motif of the COOH-terminus. Sequences were aligned with Pileup of the GCG package (Version 10) and displayed by interface of MacBoxshade 2.15. (C) *grl*<sup>m145</sup> mutation changes T to A, with a predicted effect of changing the stop codon to Gly and extending the protein by 44 amino acids at the COOH-terminus. The mutation was found in the genomic region of all eight *grl* mutant embryos examined and also found in reverse transcription-PCR of cDNA from a pool of 10 mutant embryos. Abbreviations for the amino acid residues are as follows: A, Ala; C, Cys; D, Asp; E, Glu; F, Phe; G, Gly; H, His; I, Ile; K, Lys; L, Leu; M, Met; N, Asn; P, Pro; Q, Gln; R, Arg; S, Ser; T, Thr; V, Val; W, Trp; and Y, Tyr.

## REPORTS

single-strand length polymorphism (SSLP) markers and random amplified polymorphic DNAs (4, 5), and then generated a physical map of the region using yeast artificial chromosomes (YACs) (6), bacterial artificial chromosomes (BACs), and P1 bacteriophage chromosomes (PACs) (7) (Fig. 1). Fine mapping, using recombination frequency among 2400 meioses, permitted us to refine the interval to 120 kb on overlapping BAC14 and PAC14 (Fig. 1) (8). We used two strategies to define genes within this interval. First, we assembled the sequences of BAC14 and PAC14 (9), which we analyzed by the Phred/Phrap/Consed program (9, 10), and thereby established 11 sequence contigs. Combinatory Genescan (11) and Blast Search (12) identified exons, introns, and exon-intron boundaries, with four genes (termed genes A to D). Second, we used the BAC and PAC as probes to screen embryonic cDNA libraries (13). This method identified only gene B. Subsequent fine mapping, with single-nucleotide polymorphisms, showed gene B to be outside of the *grl* region. We sequenced the other three genes from wild-type and mutant embryos and examined their expression patterns. Gene C appears to be a zebrafish ortholog of human *Pex7* (14), and gene D appears to be novel. No consistent mutations were found in the exons and exon-intron boundaries of genes C and D in mutant embryos, and the genes were not expressed in the aorta or surrounding tissues. Gene A, in

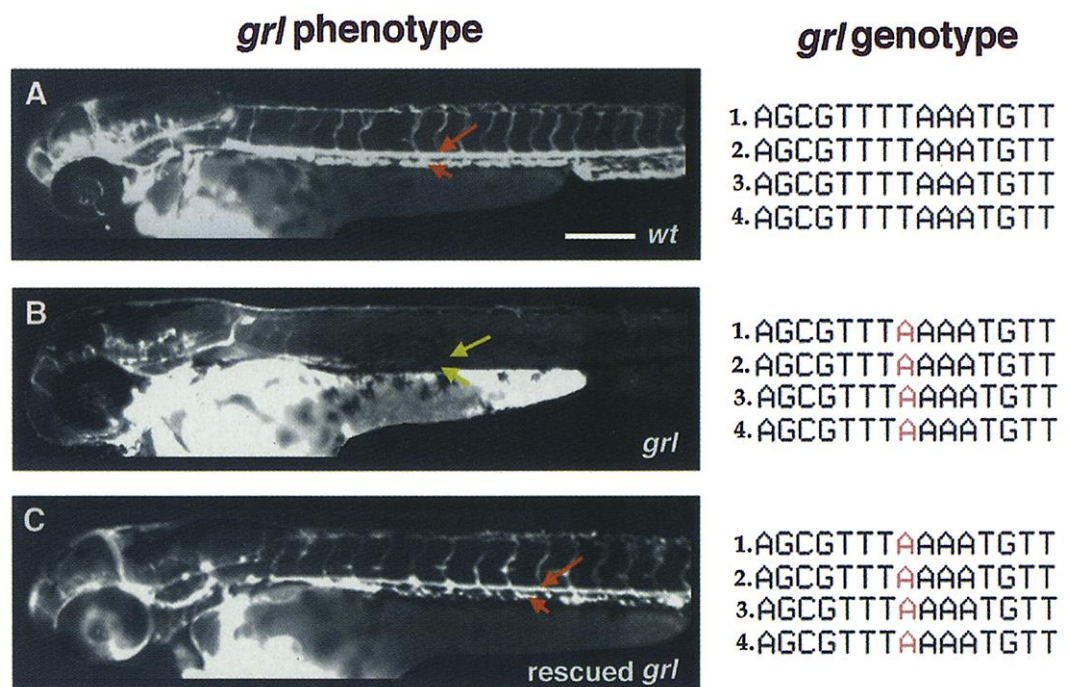
contrast, was expressed selectively in the aorta and contains a mutation in the mutant embryos (see below), leading us to conclude that it is the *grl* gene.

Conceptual translation of *grl* genomic DNA and cDNA sequences predicts a basic helix-loop-helix (bHLH) protein with an apparent human ortholog (Fig. 2A). These *grl* genes are highly related to the mouse *Hey2/HRT-2* gene (15, 16), which belong to the family of *Hairy/Enhancer-of-split related (Hesr)* bHLH genes (Fig. 2B) (17). The *Hesr* genes are a subgroup of the *Hairy*-related bHLH genes, whose function is unknown (17). Like other *Hairy* genes (18), they are predicted to encode an NH<sub>2</sub>-terminal bHLH domain, an Orange domain (19), and a protein-protein interaction motif near the COOH terminus (Fig. 2B). This COOH-terminal motif is critical for action of *Hairy* proteins, but is divergent in *Hesr* proteins (17). Among the elements that distinguish *Hesr* proteins from other members of the *Hairy*-related family are a Pro→Gly substitution in the basic domain and a change in the COOH-terminal WRPW domain to YRPW, the latter embedded within a 13-amino acid *Hesr* motif (Fig. 2B) (17). Alignment of the predicted human and zebrafish *Grl* amino acid sequences predicts 78% overall identity, 100% identity in the bHLH domain, and 95% identity in the Orange domain (Fig. 2A). The similarity between *Grl* and other *Hesr* proteins is 85% in the bHLH domain, but only 55% in the Or-

ange domain and 21% outside the conserved domains (Fig. 2B). The Orange domain confers specificity among members of the *Hairy* family (19), and the *Grls* and *Hesrs* show characteristic sequence differences in this domain (Fig. 2B). These results suggest that the *Grl* proteins are a distinct subgroup of the bHLH-YRPW family.

The genomic sequence of *grl* in mutant embryos contains a T-to-A transversion (Fig. 2C) that would change the stop codon to Gly and extend the protein by 44 amino acids. To confirm that this mutation is responsible for the mutant phenotype, we attempted to rescue the mutant embryos by injecting them with wild-type *grl* RNA. *grl<sup>m145</sup>* is a fully penetrant recessive mutation, and the most robust phenotype is absence of demonstrable circulation to the trunk at 48 hours post fertilization (hpf), as shown by microangiogram (Fig. 3, A and B). We injected one- to four-cell stage embryos from *grl<sup>m145</sup>/+* in-crosses with in vitro-transcribed *grl* RNA (20). At 48 hours, each injected embryo was examined and genotyped by using a closely linked SSLP marker. Wild-type *grl* RNA (*grl<sup>wt</sup>*) rescued 26% of genotypically mutant embryos (of 39 genotypically mutant embryos injected, 10 were phenotypically wild type) (21). We confirmed that four of these phenotypically wild-type embryos were genetically mutant by sequence analysis (Fig. 3C). Mutant *grl* RNA (*grl<sup>mut</sup>*) rescued only 5% (of 37 injected genotypically mutant embryos, 2

**Fig. 3.** Phenotypic complementation of the zebrafish *grl* mutation. (A) Phenotype of wild-type zebrafish embryos by microangiogram, revealing robust blood flow to the trunk through the dorsal aorta (long arrow), with return through the axial vein (short arrow). (B) Microangiogram of a *grl* mutant showing absence of trunk circulation, because of the blockage at aortic junction of the paired dorsal aortae (arrows point to position where the vessels would be in the wild type). Fluorescent dextran accumulates over the yolk because of the circulatory blockade. (C) After injection, some genotypically mutant embryos become phenotypically wild type. The microangiogram shows relatively complete restoration of trunk circulation through the dorsal aorta (long arrow) and axial vein (short arrow). The COOH-terminal sequence of the *grl* gene is shown to the right in four wild-type, four mutant, and four rescued embryos. (These were selected for sequence confirmation, but had already been genotyped by a closely linked marker.) The *grl* mutant embryos and the rescued *grl* mutant embryos have a T-to-A point mutation, compared with the wild-type sequence. Capped *grl* RNA was injected at the one- to



four-cell stage into wild-type and mutant embryos. Phenotypic analysis was carried out by phase contrast, and in a few cases, as shown, by angiographic analysis (3), for the presence or absence of trunk circulation at 48 hpf. Bar, 100 μm.

## REPORTS

were phenotypically wild type) (21). This is compatible with the mutation being hypomorphic rather than null (i.e., reducing rather than abolishing protein function).

In Hairy-related proteins, the COOH-terminus is the site of interaction with the transcriptional corepressor Groucho (22). It is conceivable that the mutation-induced protein extension interferes with the function of this region. Consistent with this hypothesis, *grl* mRNA lacking the YRPW domain (*grl<sup>del</sup>*) was unable to rescue the mutant phenotype when injected into genotypically mutant embryos (0 of 38 embryos rescued) (21).

In gene expression analyses, the *grl* transcript is detected as bilateral mesodermal stripes as early as the 10-somite stage in zebrafish embryos, before vessel formation (Fig. 4A) (23). Thereafter, some of *grl*-expressing cells appear to converge toward the midline to form the primordium of the dorsal

aorta at the 24-somite stage (Fig. 4D). By the 30-somite stage, when blood flow begins, *grl* is expressed strongly throughout the dorsal aorta, including the trunk region (Fig. 4, B, C, F, and G) and anterior bifurcation (Fig. 4, E and J). No *grl*-expressing cells are observed in the region of the axial vein, ventral to the aorta (Fig. 4, D, F, and G). In contrast, *fli* (24), an early endothelial marker, is expressed both in arteries and veins (Fig. 4, H and I). In addition, *grl* is transiently expressed in the heart, aortic arches, and lateral somites, a pattern similar to that described for the mouse *Hey* and *HRT* genes (15, 16).

It is not known how or when angioblasts assume a particular vascular fate in the early embryo. Nor is it known which genes drive vessels to assemble into tubes of a particular branching form. The finding of *grl* as a member of a bHLH transcriptional regulatory gene family, and as a gene needed for proper formation

of the aorta, speaks to issues of both angioblast cell fate and vascular morphogenesis.

Grl is a member of the Hairy-related family of bHLH proteins, which are important for cell fate determination in other cell types (25). In the *Drosophila* nervous system, for example, members of the Hairy family act downstream of Notch as transcriptional repressors and help to "single out" neuronal precursor cells within "equivalence groups" (25). We speculate that Grl plays a similar role specifically for aortic angioblasts and that other bHLH proteins may be required for specification of vein angioblasts. Different bHLH proteins, including stem-cell leukemia/T-cell acute leukemia 1, Tfeb, hypoxia-inducible HIF-1 $\alpha$  and HIF-2 $\alpha$ , and the dominant inhibitory HLH factors Id1 and Id3, are involved in a variety of endothelial functions (26), including angiogenesis, but no bHLH proteins have been clearly linked to vasculogenesis. Vascular endothelial growth factor (Vegf) and its receptor Flk are essential for early vasculogenesis (1, 27), and it will be important to determine whether Grl functions in the Vegf/Flk pathway.

Although *grl* is expressed throughout the entire vessel, the most anterior region of the aorta, the bifurcation, is particularly affected in the mutant. This may be due to the fact that the mutation reduces but does not eliminate Grl function. Perhaps other genes provide redundant function in the other regions of the aorta. Indeed, three related *Hey* and *HRT* genes are expressed in the mammalian aorta (15, 16). The aortic bifurcation is particularly susceptible to congenital dysmorphogenesis in humans, suggesting that it may be more sensitive than the rest of the aorta to perturbation. Some of these clinical disorders, such as coarctation, show a high sibling recurrence (28), and it will be of interest to examine *grl* as a candidate gene for these diseases.

Zebrafish mutations are proving to be especially informative about vertebrate-specific processes, such as organogenesis. The hope of the zebrafish genetic screens was that they would not only inform about the logic of development, and the role of known genes, but also lead to discovery of novel genes. As exemplified here by *grl*, and by *oep* (29) and *weh* (30), the positional cloning infrastructure for zebrafish now is sufficiently robust to make this a reality.

### References and Notes

1. W. Risau, *Nature* **386**, 671 (1997).
2. H. U. Wang, Z. Chen, D. J. Anderson, *Cell* **93**, 741 (1998).
3. B. M. Weinstein, D. L. Stemple, W. Driever, M. C. Fishman, *Nature Med.* **1**, 143 (1995).
4. J. H. Postlethwait et al., *Science* **264**, 699 (1994).
5. N. Shimoda et al., *Genomics* **58**, 219 (1999).
6. T. P. Zhong et al., *Genomics* **48**, 136 (1998).
7. C. T. Amemiya, T. P. Zhong, G. A. Silverman, M. C. Fishman, L. I. Zon, in *The Zebrafish—Genetics and Genomics*, H. W. Detrich III, M. Westerfield, L. I. Zon, Eds. (Academic Press, San Diego, CA, 1999), p. 236.

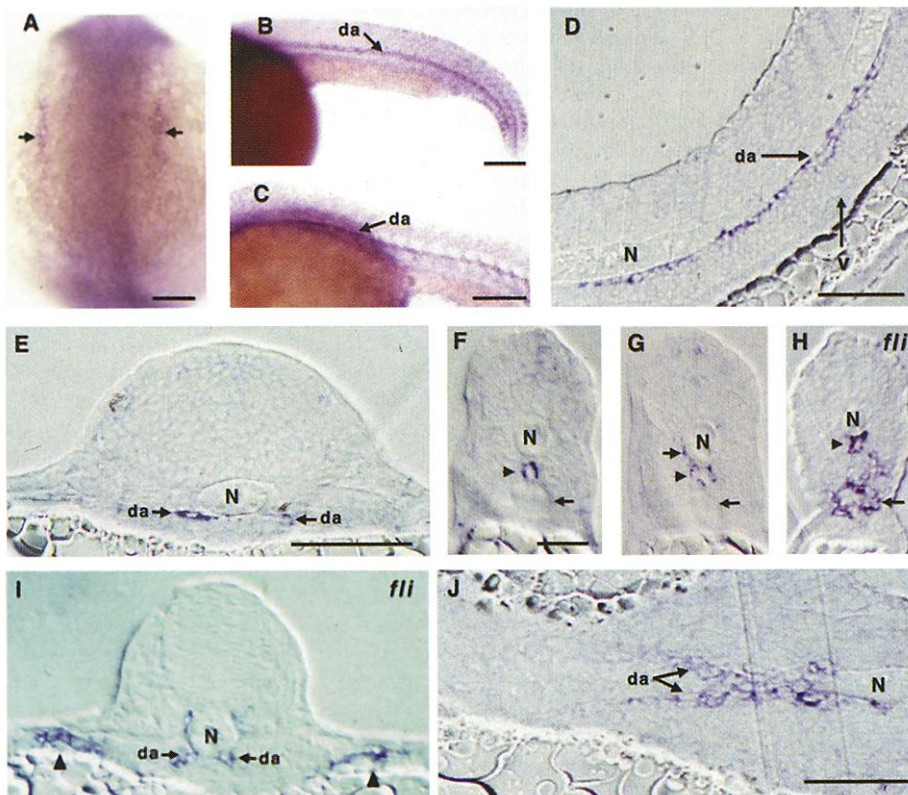


**Fig. 4.** Expression of *grl* mRNA in zebrafish. (A) *grl* is expressed as bilateral stripes at lateral plate mesoderm (arrows) at the 10-somite stage (dorsal view). (B and C) Lateral views of the anterior trunk, posterior trunk, and tail, showing *grl* transcripts in the dorsal aorta (arrows). (D) Sagittal section of the posterior trunk showing *grl* expression in the primordium of dorsal aorta (arrow), but not in the axial vein (arrowhead) at the 24-somite stage. (E) Transverse section of the anterior trunk, showing *grl* expression in the paired dorsal aortae (arrows) ventral to the notochord, but not in the bilateral cardinal veins [see arrowheads in (I)]. (F and G) Transverse section of posterior trunk, showing *grl* expression in the dorsal aorta (arrowhead) beneath the notochord, and extending into what is likely a sprout (intersomatic artery) (short arrow), but not in the axial vein (arrow). (H) *fli* expression highlights both the axial vein (arrow) and the dorsal aorta (arrowhead) in the posterior trunk. (I) Transverse section through the anterior trunk at the level of the first somite. *fli* is expressed in the bilateral common cardinal veins (arrowheads) and the paired dorsal aortae (arrows). (J) Longitudinal section of the anterior trunk showing a dorsal view of *grl* expression in the aortic bifurcation. Dorsal is up in (B) to (I), anterior is to the left in (B), (C), and (J). The in situ hybridization was carried out at the 30-somite (24 hours) stage (B, C, E to I, J). N, notochord; da, dorsal aorta; v, vein. Bars, 100  $\mu$ m (A, B, C, D, and J), 50  $\mu$ m (E and I), and 50  $\mu$ m (F to H).

8. Recombinant fine mapping analysis was performed with single-stranded conformation polymorphisms from the sequence of rescued YAC, BAC, and PAC ends. The YAC ends were rescued by self-circularization, and the BAC/PAC ends were rescued by inverse polymerase chain reaction (PCR) or directly sequenced.

9. Genomic DNA shotgun libraries of BAC14 and PAC14 were made by shearing DNA with a Sonic Dismembrator (20.3 cm by 30.5 cm) (Fisher Scientific) and digesting the DNA with mung bean nuclease. The DNA was then size-selected on agarose gel and blunt-end ligated. High-throughput DNA preps were performed with Qiagen Robot 9600. Shotgun sequencing, estimated to provide fivefold genomic DNA sequence coverage of BAC14 and PAC14, was carried out with an ABI 377 (Perkin Elmer). About 2000 genomic sequences were analyzed with the Phred program. The flanking sequence of the vector was clipped off with CrossMatch. The sequence contigs were assembled with Phrap and edited by Consed.

10. D. Gordon, C. Abajian, P. Green, *Genome Res.* **8**, 195 (1998).

11. C. B. Burge, in *Computational Methods in Molecular Biology*, S. Salzberg, D. Searls, S. Kasif, Eds. (Elsevier, Amsterdam, 1998), p. 127.

12. S. F. Altschul et al., *Nucleic Acids Res.* **25**, 3389 (1997).

13. Filters of a 24 hpf embryonic cDNA library were screened with  $\alpha^{32}$ -P-labeled BAC14 or PAC14, which was first annealed in a genomic repeats repressing mixture [ $5\times$  SSC genomic DNA (2.5  $\mu$ g/ $\mu$ l), CA and GT oligonucleotide (0.5  $\mu$ g/ $\mu$ l each), and mermaid repeats (0.5  $\mu$ g/ $\mu$ l each)] in hybridization buffer [ $6\times$  SSC, 0.5% SDS, calf thymus DNA (100  $\mu$ g/ $\mu$ l)] overnight. The filters were then washed in  $2\times$  SSC-0.1% SDS,  $0.2\times$  SSC-0.1% SDS.

14. P. E. Purdue, J. W. Zhang, M. Skoneczny, P. B. Lazarow, *Nature Genet.* **15**, 381 (1997).

15. C. Leimeister, A. Externbrink, B. Klamat, M. Gessler, *Mech. Dev.* **85**, 173 (1999).

16. O. Nakagawa, M. Nakagawa, J. A. Richardson, E. N. Olson, D. Srivastava, *Dev. Biol.* **216**, 72 (1999).

17. H. Kokubo, Y. Lun, R. L. Johnson, *Biochem. Biophys. Res. Commun.* **260**, 459 (1999).

18. I. Palmeirim, D. Henrique, D. Ish-Horowitz, O. Pourquie, *Cell* **91**, 639 (1997).

19. S. R. Dawson, D. L. Turner, H. Weintraub, S. M. Parkhurst, *Mol. Cell. Biol.* **15**, 6923 (1995).

20. Sense-capped RNA was synthesized for injection with T7 RNA polymerase and the mMACHINE mMACHINE system (Ambion) after Hind III digestion of *grl* wild type, *grl* mutant with COOH-terminal extension, and *grl* deletion bearing the COOH-terminal truncation. Injection was carried out with a Microinjector 5242 (Eppendorf, Germany).

21. Embryos obtained from *grl*<sup>m145</sup> heterozygote in-crosses were injected with capped in vitro-transcribed *grl* RNA, of one of three types: wild-type sequence; *grl* mutant sequence (i.e., with COOH-terminal extension); or truncated at amino acid position 250 before the YRPW motif. Various dosages of mRNA were tested. About 55 pg of RNA was used for these experiments. An average of 90% of wild-type embryos injected with 55 pg of *grl*<sup>wt</sup>, *grl*<sup>mut</sup>, or *grl*<sup>del</sup> RNA develop normally. High dosages (about 200 pg) cause more widespread developmental defects in about 60% of embryos.

22. A. L. Fisher, S. Ohsako, M. Caudy, *Mol. Cell. Biol.* **16**, 2670 (1996).

23. For whole-mount RNA in situ hybridization, a 1891-bp fragment of cDNA was subcloned for in vitro transcription. For histological analysis, specimens were fixed in 4% paraformaldehyde, dehydrated, and embedded in plastic (JB-4). Nomarski photomicroscopy was performed with an Axiophot with Ektachrome 160T film (Zeiss). Wild M5 and M10 dissecting microscopes equipped with Nikon cameras were used for low-power photomicroscopy.

24. M. A. Thompson et al., *Dev. Biol.* **197**, 248 (1998).

25. S. Artavanis-Tsakonas, M. D. Rand, R. J. Lake, *Science* **284**, 770 (1999).

26. P. Carmeliet, *Nature* **401**, 657 (1999).

27. W. Liao et al., *Development* **124**, 381 (1997).

28. M. E. Pierpont and J. Moller, in *Genetics of Cardiovascular Disease*, M. E. Pierpont and J. H. Moller, Eds. (Nijhoff, Boston, MA, 1986), p. 13.

29. J. J. Zhang, W. S. Talbot, A. F. Schier, *Cell* **92**, 241 (1998).

30. A. Donovan et al., *Nature* **403**, 776 (2000).

31. We thank X. Kue, S. Sanghvi, S. Childs, M. Yasuda, and C. Simpson for help with DNA sequencing and other

technical assistance, and D. Ransom and L. Zon for the *Fli* probe. T.P.Z. is supported by NIH training grant T32HL07208. Supported in part by NIH grants R01RR0888, R01DK55383, and R01HL49579 (M.C.F.) and a sponsored research agreement with Genentech (M.C.F.).

11 November 1999; accepted 21 January 2000

## DNA Damage-Induced Activation of p53 by the Checkpoint Kinase Chk2

Atsushi Hirao,<sup>1</sup> Young-Yun Kong,<sup>1</sup>

Suhei Matsuoka,<sup>2</sup> Andrew Wakeham,<sup>1</sup> Jürgen Ruland,<sup>1</sup>

Hiroki Yoshida,<sup>1\*</sup> Dou Liu,<sup>2</sup> Stephen J. Elledge,<sup>2</sup> Tak W. Mak<sup>1†</sup>

Chk2 is a protein kinase that is activated in response to DNA damage and may regulate cell cycle arrest. We generated Chk2-deficient mouse cells by gene targeting. Chk2<sup>-/-</sup> embryonic stem cells failed to maintain  $\gamma$ -irradiation-induced arrest in the G<sub>2</sub> phase of the cell cycle. Chk2<sup>-/-</sup> thymocytes were resistant to DNA damage-induced apoptosis. Chk2<sup>-/-</sup> cells were defective for p53 stabilization and for induction of p53-dependent transcripts such as p21 in response to  $\gamma$  irradiation. Reintroduction of the Chk2 gene restored p53-dependent transcription in response to  $\gamma$  irradiation. Chk2 directly phosphorylated p53 on serine 20, which is known to interfere with Mdm2 binding. This provides a mechanism for increased stability of p53 by prevention of ubiquitination in response to DNA damage.

The maintenance of genomic integrity after DNA damage depends on the coordinated action of the DNA repair system and cell cycle checkpoint controls. The failure of such controls leads to genomic instability and a predisposition to cancer (1). Chk2 is a mammalian homolog of the *Saccharomyces cerevisiae* Rad53 and *Schizosaccharomyces pombe* Cds1 checkpoint genes. Chk2 is a protein kinase that acts downstream of ataxia telangiectasia mutated (ATM) and may regulate cell cycle arrest (2-4).

To investigate the physiological role of Chk2, we generated Chk2-deficient cells by gene targeting in embryonic stem (ES) cells (5). The genotype of Chk2<sup>-/-</sup> ES clones was confirmed by Southern (DNA) blotting (Fig. 1A), and complete loss of Chk2 protein in Chk2<sup>-/-</sup> cells was confirmed by protein immunoblotting (Fig. 1B) (6). Because Chk2 is thought to have a role in the prevention of entry into mitosis

(2-4), we examined arrest of the cell cycle in ES cells, a cell type in which  $\gamma$  irradiation induces arrest in the G<sub>2</sub> phase but not arrest in the G<sub>1</sub> phase or apoptosis (7). Twelve hours after 10 grays (Gy) of  $\gamma$  irradiation, about 90% of both Chk2<sup>+/+</sup> and Chk2<sup>-/-</sup> ES cells were arrested with a G<sub>2</sub> DNA content (Fig. 1C). However, at later time points, substantially more Chk2<sup>-/-</sup> cells entered G<sub>1</sub> and S relative to controls. Examination of only S phase cells marked by a bromodeoxyuridine (BrdU) pulse label gave similar results (Fig. 1C, middle panel). We additionally investigated whether cells were able to enter M phase after  $\gamma$  irradiation by treatment with nocodazole, a microtubule-disrupting agent that traps cells in mitosis (8, 9). In the absence of  $\gamma$  irradiation, about 35% of cells of both genotypes were trapped in mitosis after 12 hours of nocodazole treatment (Fig. 1D). When cells were subjected to  $\gamma$  irradiation with nocodazole treatment, cells of both genotypes arrested in G<sub>2</sub> for 12 hours (Fig. 1D). However, after 18 hours, significantly more Chk2<sup>-/-</sup> cells entered mitosis. p53<sup>-/-</sup> ES cells did not show a defect in cell cycle arrest after  $\gamma$  irradiation (Fig. 1C), as previously shown (7), indicating that the defect in G<sub>2</sub> arrest observed in Chk2<sup>-/-</sup> ES cells is p53-independent.

Consistent with these results, asynchronous cells irradiated with 10 Gy showed a reduction in Cdc2-associated H1 kinase activity after 12 hours. However, Chk2<sup>-/-</sup> cells were unable to maintain this reduction (Fig. 1E). These results indicate that Chk2 is required for the mainte-

<sup>1</sup>The Amgen Institute, Ontario Cancer Institute, and Departments of Medical Biophysics and Immunology, University of Toronto, 620 University Avenue, Suite 706, Toronto, Ontario, M5G 2C1, Canada. <sup>2</sup>Howard Hughes Medical Institute, Verna and Marrs McLean Department of Biochemistry and Molecular Biology, and Department of Molecular and Human Genetics, Baylor College of Medicine, One Baylor Plaza, Houston, TX 77030, USA.

\*Present address: Department of Immunology, Medical Institute of Bioregulation, Kyushu University, 3-1-1 Maidashi, Higashi-Ku, Fukuoka 812-8582, Japan.

†To whom correspondence should be addressed. E-mail: tmak@oci.utoronto.ca